Ibn Al-Haitham Journal for Pure and Applied Sciences
Journal homepage: jih.uobaghdad.edu.iq
PISSN: 1609-4042, EISSN: 2521-3407
IHJPAS. 2025, 38 (1)

# Preparation and Study Annealing Effect on Structure and Optical Properties of $ZnIn_2(Se_{0.8}Te_{0.2})_4$ Thin Film

**Husham Kamil Mahmood[1] and Bushra H. Hussein[2*]**
[1,2]Department of Physics, College of Education for Pure Science (Ibn Al-Haitham), University of Baghdad, Baghdad, Iraq.
*Corresponding Author.

Received: 7 April 2024 Accepted: 20 August 2024 Published: 20 January 2025
doi.org/10.30526/38.1.3982

## Abstract

The thermal evaporation technique is used to investigate the structural and optical properties of $ZnIn_2(Se_{1-0.2}Te_{0.2})_4$ (ZIST) chalcopyrite semiconductors. $ZnIn_2(Se_{0.8}Te_{0.2})_4$ thin films with a thickness of 500 nm are taken into consideration, and the effect of annealing at various temperatures ranged from R.T, 373, 473 K. (ZIST) Thin film is widely regarded as a remarkable semiconductor material for the development of second-generation solar cells. $ZnIn_2(Se_{0.8}Te_{0.2})_4$ films are polycrystalline with excellent stoichiometric composition, as shown by XRD and AFM investigations. According to a structural study, annealing the films after they were deposited increased the average grain size and crystallite size after annealing, as well as one of the favored orientations of the polycrystalline phase is along the (112) direction. The wavelength range used to determine these films' optical characteristics was 400 nm–1000 nm. Semiconductors $ZnIn_2(Se_{1-0.2}Te_{0.2})_4$ have direct band gaps of 1.7, 1.65, and 1.6 eV respectively. The calculated optical constant includes the refractive index. extinction coefficient. real and imaginary components of dielectric constant.

**Keywords:** Chalcopyrite semiconductors, XRD, band gaps $ZnIn_2(Se_{1-0.2}Te_{0.2})_4$, thin film.

## 1. Introduction

$ZnIn_2Se_4$ is important semiconductor compounds with the composition II-III2-VI4 (where II=zinc (Zn), mercury Hg or cadmium (Cd); III is aluminum (Al), indium In or gallium (Ga), VI= Selenium Se, Sulphur S or Tellurium Te)(1) These have been extensively studied because of their possible uses as temperature sensors, IR detectors (2) photoconductors, narrow-band optical filters (3) solar cell (4) $ZnIn_2Se_4$ has garnered significant attention because to its comparatively elevated photo electrochemical sensitivity across the visible to near-infrared spectral range. and also promising material for optoelectronic applications (5) The properties of

these materials can be controlled and optimized through $ZnIn_2Se_4$ various synthesis methods such as flash evaporation (6) plasmon resonances (7) thermal evaporation in vacuum (8) spray pyrolysis technique (9) Bridgman technique (10) Chemical Bath Deposition (11) electrodeposition method (12) Chemical vapor transport (13) The structure of $ZnIn_2Se_4$ thin films has a lattice parameter of a=5.7095 Å and c=11.449Å and a tetragonal crystal structure (8,13). The band gap of $ZnIn_2Se_4$ is around 1.5 to 2.2 electron volts (eV). This range places it in the visible to near-infrared (NIR) regions of the electromagnetic spectrum. The direct bandgap nature of $ZnIn_2Se_4$ allows for efficient absorption and emission of light, making it suitable for various optoelectronic applications (14) $ZnIn_2Se_4$ is a semiconductor, electrical conductivity can be modified by doping with other elements or by changing the stoichiometry during synthesis (15) $ZnIn_2Se_4$ non-toxic and P-type semiconductor (4,6) N-type, direct band gap semiconductor (1). Numerous research has looked at the effects of various doped materials on the characterization of $ZnIn_2Se_4$ such as the influence of (Co) doping (10) Cu doping with ratio 2.67 on Photoconductivity properties Bridgman method (16,17) Mn on structural and electronic properties (1) carrier concentration of $2.8\times10^{18}$ $cm^{-3}$ (18) ($8.854\times10^{14}$ F/cm) $\varepsilon_r$ is the relative dielectric constant values of the $ZnIn_2Se_4$ (6) absorption coefficient of $5.3 \times 10^{\wedge 6}$ $cm^{-\wedge 1}$ in the visible regions (19).

In this work, $ZnIn_2(Se_{1-0.2}Te_{0.2})_4$ where x = 0.2 thin films are fabricated using the vacuum evaporation method, and the effects of annealing at (473, 573) K are examined concerning their optical measurement, XRD, AFM, and the relationship between these parameters.

## 2. Materials and Methods

A thin film of zinc, indium, selenium, and tellurium alloys has been manufactured. The stoichiometric weight ratios (1:2:0.8:0.2) and high elemental purity (99.99%) of the ZIST elements were combined. The resulting alloy was subjected to a pressure of $5\times10^{-3}$ mbar in quartz tubes, followed by six hours of heating in an electric oven at 1273 K. It is worth noting that the temperature required to fully solidify the alloy exceeded the melting point of $ZnIn_2Se_4$ and $ZnIn_2Te_4$ [20]. To investigate the optical and structural properties of ZIST thin films, they were the material is applied onto glass substrates. at a relative humidity (RT) of $4.5 \times10^{-5}$ Torr to produce a 500 nm thick film with good uniformity, adhesion to the substrate, and absence of cracks. X-ray diffraction XRD, AFM have been utilized to define the structural morphology of ZIST films. The structure of these films was investigated using X-ray diffraction & Scherer's Formula was utilized to compute their crystalline dimension (21, 22).

$$C.S = \frac{0.9\lambda}{\beta\cos\theta} \quad (1)$$

The symbol $\beta$ represents the diffraction width of the peaks at half maximum (FWHM), the crystallite size (C.S), (θ) is the diffraction peak angle.

The determination of the lattice constant a & c for a tetragonal structure is accomplished via the following equation (23):

$$\frac{4sin^2\theta}{\lambda^2} = \frac{h^2+k^2}{a^2} + \frac{l^2}{c^2} \quad (2)$$

Where Miller incidents (hkl). The calculation of (Ɛ) microstrain for manufactured thin film can be determined using the following:

$$\text{Ɛ} = \frac{\beta \cos\theta}{4} \quad (3)$$

The density of dislocations (δ) is the ratio of the lengths of the dislocation line to the crystal volume. It may be calculated using the following (24):

$$\delta = \frac{1}{(C.S)^2} \quad (4)$$

To determine the energy gap, Measurements of optical transmission within the wavelength range of 400-1000 nm were performed. Optical characteristics of the thin film preparation have been observed through transmission and absorption spectra spanning a wavelength range of 400 to 1000 nanometers. The energy gap ($E_g$) from the absorption spectrum has been computed using the Lambert law and Tauc equations, respectively (25,26):

$$\alpha = 2.303 \frac{\text{A}}{t} \quad (5)$$

$$\alpha h\upsilon = D\,(h\upsilon - E_g)^r \quad (6)$$

the precise value of the constant D that is temperature dependent. The absorption coefficient is denoted by the symbol $\alpha$, hυ signifies the magnitude of the incident photons' energy and r is a factor that specifies the optical transition type. Absorption (A) and thickness (t).

The following relationships can be used to calculate optical constants, including the extinction coefficient k the refractive index n the real part $\varepsilon_r$, and the imaginary part $\varepsilon_i$ of the dielectric constant, the reflection R(27-29):

$$k = \frac{\alpha\,\lambda}{4\pi} \quad (7)$$

$$n = \left[\frac{4R}{(1-R)^2} - k^2\right]^{1/2} - \frac{(1+R)}{(1-R)} \quad (8)$$

$$\varepsilon_i = 2nk \quad (9)$$

$$\varepsilon_r = n^2 - k^2 \quad (10)$$

## 3. Results and Discussion

The X-ray diffraction patterns of $ZnIn_2(Se_{0.8}Te_{0.2})_4$ thin films, measuring 500 nm in thickness, were observed at room temperature (R.T) & (373,473) K. The pattern indicates that both the pre-annealed and annealed thin films possess a polycrystalline structure, as evidenced by the reflection from the (112), (204), and (312) planes, which correspond to tetragonal structures. Furthermore, the films exhibit a distinct growth direction corresponding to the plane (112). Each peak of the diffraction can be attributed to the ternary compound $ZnIn_2Se_4$, JCPDS file no. 00-039-0458 card standard value. Upon annealing at temperatures of 373 and 473 K, the location of the observed diffraction peaks exhibits no alteration. substantially, however, the intensities of the peak increased and the size of the crystallites grew. This suggests that the quality of crystalline films has been enhanced as a result of reduced defects and system regularity (30). By analyzing the FWHM values of the (112) peak in the thin films illustrated in **Figure 1**, the crystallite size

can be estimated using Scherrer's equation. The data presented in **Table 1** reveals that when annealing temperatures are increased for ZnInSeTe, there is an increase in crystallite size, suggesting a higher likelihood of material crystallization in the films, and the values of lattice constants a = 5.7095 Å & c = 11.449Å is very close to research (8,13). The optical, electrical, and thermoelectric properties of $ZnIn_2(Se_{0.8}Te_{0.2})_4$ (at $T_a$ = 473 K) thin films are significantly influenced by their high degree of crystallinity. In addition to being utilized in solar cells and thermoelectric generators, the films' smooth and uniform surface is crucial for their application in a variety of technological devices.

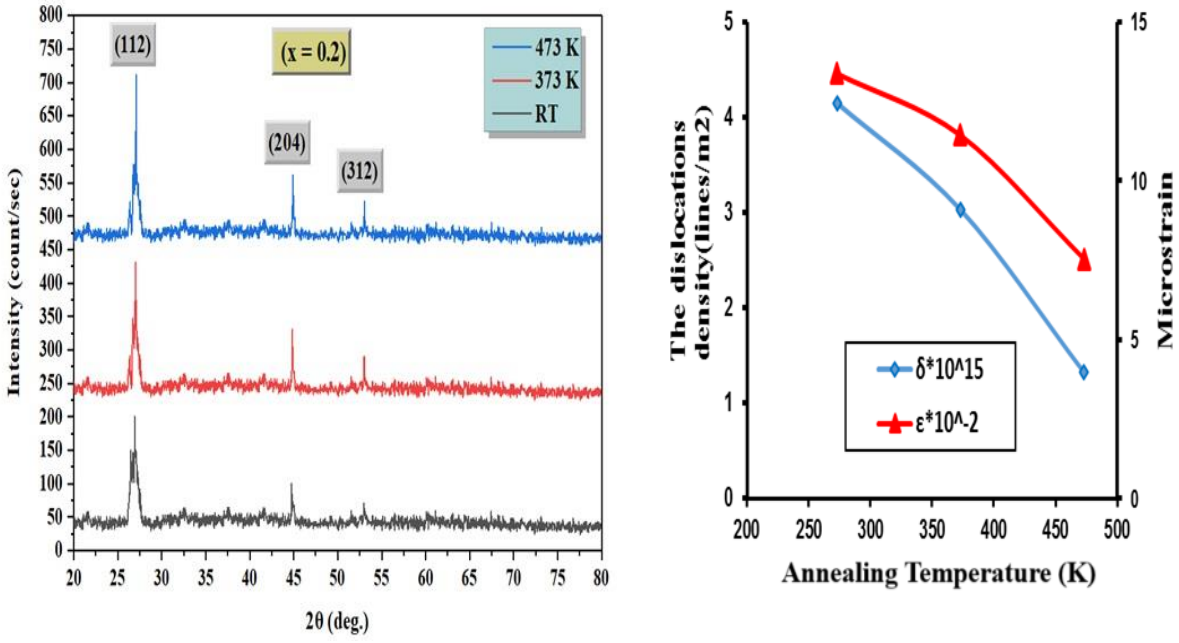


**Figure 1.** X-ray diffraction pattern for thin films $ZnIn_2(Se_{0.8}Te_{0.2})_4$ with (R.T, 373 and 473) K.

The results for micro strain and dislocation density have been computed and are presented in **Table 1.** The drop in micro strain and dislocation density is apparent as the annealing temperature increases. The observed phenomenon can be attributed to the positive correlation between micro strain and full width (FWHM) at half maximum of the primary peak, as well as the negative correlation between dislocations density and crystallite size. The observed reduction in flaws in $ZnIn_2(Se_{0.8}Te_{0.2})_4$ thin films as the annealing temperature increases suggests an enhancement in their structure of crystal.

Using AFM analysis, the surface morphology of $ZnIn_2(Se_{0.8}Te_{0.2})_4$ thin film with temperatures equal R.T, 373 and 473 K was investigated. The size distribution chart and three-dimensional AFM image of these films are displayed in **Figure 2.** On the surface of the substrate, minute particles have proliferated, and variations in pyramidal morphology are visible. The physical characteristics of the structure including roughness, roots mean square, and average diameter (G.S), are detailed in **Table 2.** The structures exhibited fluctuations in roughness and root mean square values, in addition to variations in average grain size (79.9-94.4 nm). The table presents

the results of annealing thin film, which indicate an increase in average particle size, roughness, and root mean square. Additionally, the sample ZIST shows a major magnitude at 473 K. This manner of behavior can be ascribed to the increased atomic mobility, which leads to the aggregation of particles, particularly larger particles. This agglomeration ultimately indicates an increase in the texture of the films. These observations corroborate the XRD findings.

**Table 1.** X-ray diffraction data from experiments for thin film $ZnIn_2(Se_{0.8}Te_{0.2})_4$ with (R.T, 373 and 473) K.

| $T_a$ (K) | $d_{exp.}$ (Å) | $2\theta_{exp}$ (deg.) | (hkl) | FWHM (deg.) | C.S (nm) | $\delta \times 10^{15}$ (lines/m$^2$) | $E \times 10^{-2}$ |
|---|---|---|---|---|---|---|---|
| R.T | 3.308 | 26.92 | (112) | 0.55 | 15.51 | 4.15 | 13.37 |
| | 2.022 | 44.76 | (204) | | | | |
| | 1.726 | 52.96 | (312) | | | | |
| 373 | 3.298 | 27 | (112) | 0.47 | 18.16 | 3.03 | 11.43 |
| | 2.018 | 44.84 | (204) | | | | |
| | 1.725 | 53 | (312) | | | | |
| 473 | 3.288 | 27.08 | (112) | 0.31 | 27.53 | 1.32 | 7.53 |
| | 2.015 | 44.92 | (204) | | | | |
| | 1.724 | 53.04 | (312) | | | | |

**Table 2.** Roughness average, grain size and root mean square of $ZnIn_2(Se_{0.8}Te_{0.2})_4$ with (R.T, 373 and 473) K.

| Thickness (500 nm) | Average diameter (nm) | Roughness average (nm) | Root mean square |
|---|---|---|---|
| R.T | 79.9 | 19.63 | 26.1 |
| 373 | 92.8 | 20.57 | 24.04 |
| 473 | 94.4 | 22.33 | 25.27 |

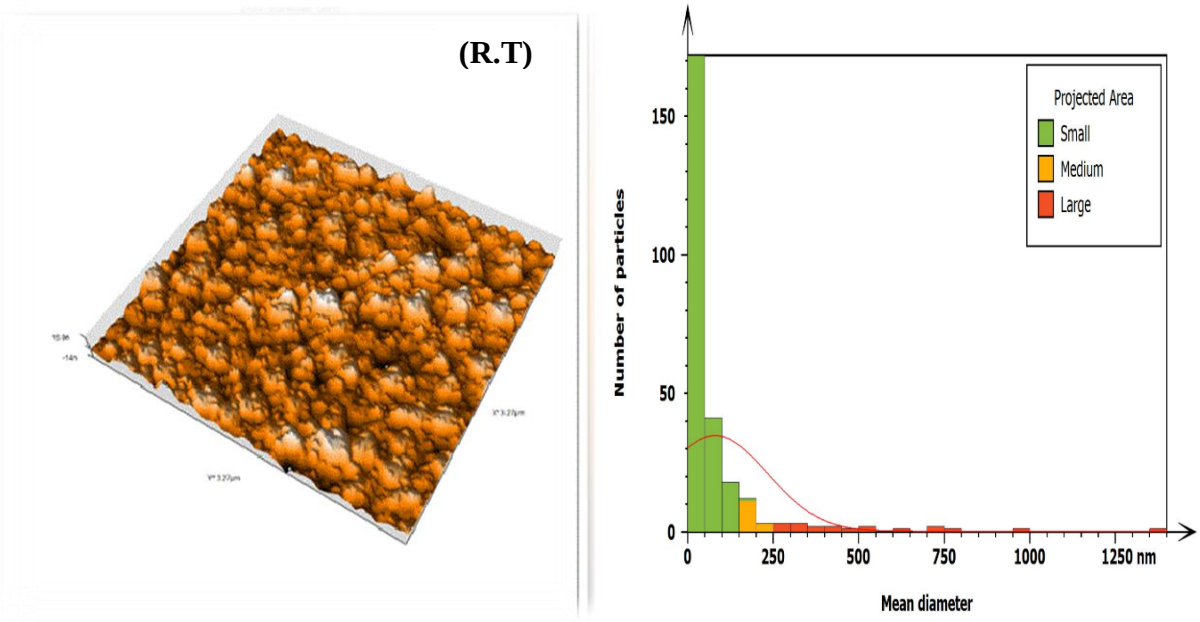

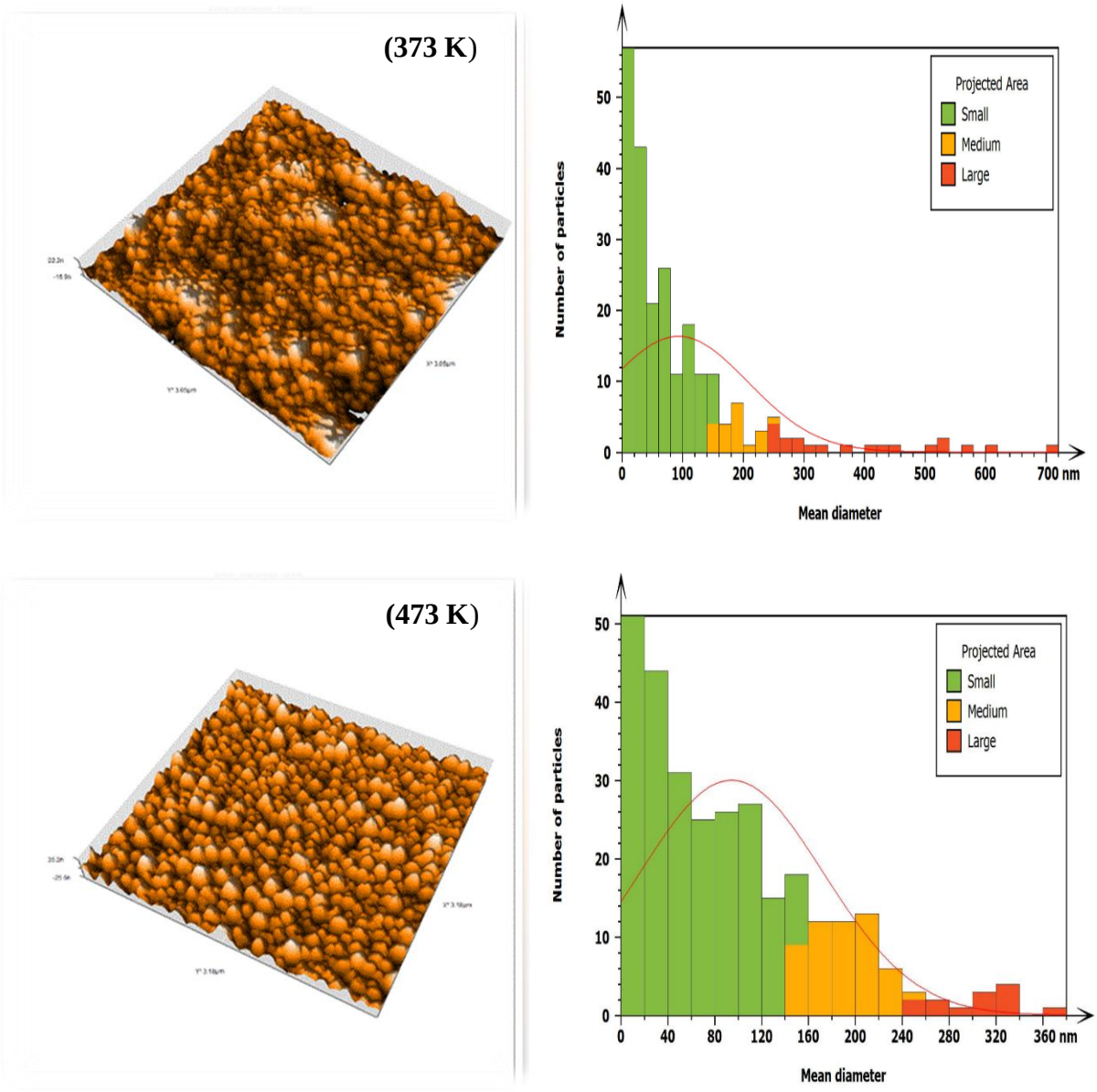


**Figure 2.** Atomic force microscope image and size distribution for $ZnIn_2(Se_{0.8}Te_{0.2})_4$ at (R.T, 373 and 473) K.

Depending on the values of absorbance and transmittance within a range (400-1000), the transmittance relationship is drawn (nm) based on the wavelength depicted in **Figure 3**, and this shows that the results of $ZnIn_2(Se_{0.8}Te_{0.2})_4$ at R.T and (373,473) K films have a high rate of absorbance about (90%) in the visible spectrum regions and with increasing annealing temperature, we notice that there is a decrease in transmittance values are offset by an increase in absorbance and deflection values fundamental absorption edge toward long wavelength (low energy), This behavior can be attributed to the utilization of X-ray diffraction (XRD) and atomic force microscopy data to comprehend the relationship between surface morphology and the observed increment in absorbance (31,32). This implies that following the annealing process, the

absorbance values of these thin films exhibit an upward trend. This increase can be attributed to the absorption of photons by free carriers, Consequently, this results in a reduction in transmittance. Alternatively, it may be linked to the development of crystallite sizes (33,34). Consequently, the potential for absorbing low-energy photons is plausible.

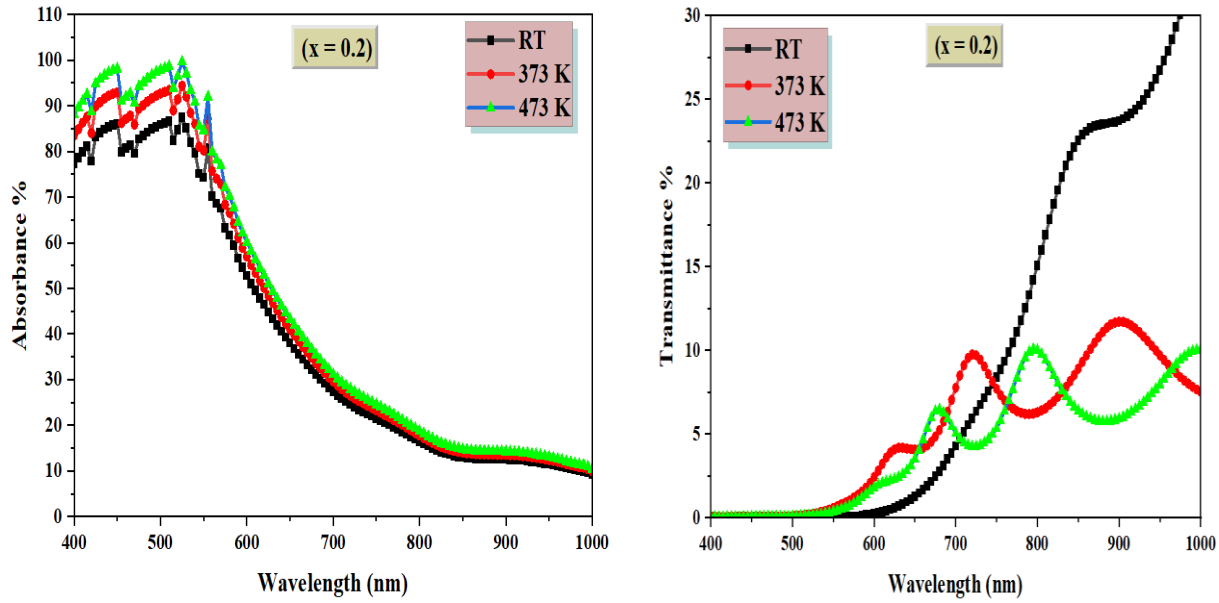


**Figure 3.** The transmittance and absorption spectrum of $ZnIn_2(Se_{0.8}Te_{0.2})_4$ with (R.T, 373 and 473) K.

The change in absorption coefficient as function of wavelengths is depicted in **Figure 4** for $ZnIn_2(Se_{0.8}Te_{0.2})_4$ film with (R.T 373 and 473) K, we note that the absorption coefficient increases gradually by a small amount with increasing photon energy, and this rapid increase helps us to determine the fundamental absorption edge, the results showed that increasing the annealing temperatures led to a clear increase in all values absorption coefficient, especially at low energies, and this It seems clear from **Figure 4**. As the edge of absorption creeps fundamentals towards lower photon energies. We also note that the absorption coefficient for all cases has values greater than $10^4$ in the high energy range, which indicates the occurrence of direct electronic transfers, and this agrees with the research (19). The energy gap was determined using the Tauc equation. The change of $E_g$ $ZnIn_2(Se_{0.8}Te_{0.2})_4$ films with (R.T, 373 and 473) K is shown in **Figure 4.** The transition was directly allowed of $ZnIn_2(Se_{0.8}Te_{0.2})_4$ film was calculated from 1.7 eV to 1.6 eV strong concurrence with (9).

**Table 3.** Optical factors ($E_g^{opt}$, α, n, k, $\varepsilon_r$ & $\varepsilon_i$) for $ZnIn_2(Se_{0.8}Te_{0.2})_4$ with (R.T, 373 and 473) K where λ = 500 nm.

| Thickness (500 nm) | $E_g^{opt}$(eV) | $\alpha \times 10^4$ ($cm^{-1}$) | n | k | $\varepsilon_r$ | $\varepsilon_i$ |
|---|---|---|---|---|---|---|
| R.T | 1.7 | 3.95 | 1.6 | 0.15 | 2.5 | 0.5 |
| 373 | 1.65 | 4.26 | 1.4 | 0.16 | 1.8 | 0.46 |
| 473 | 1.6 | 4.5 | 1.3 | 0.17 | 1.33 | 0.41 |

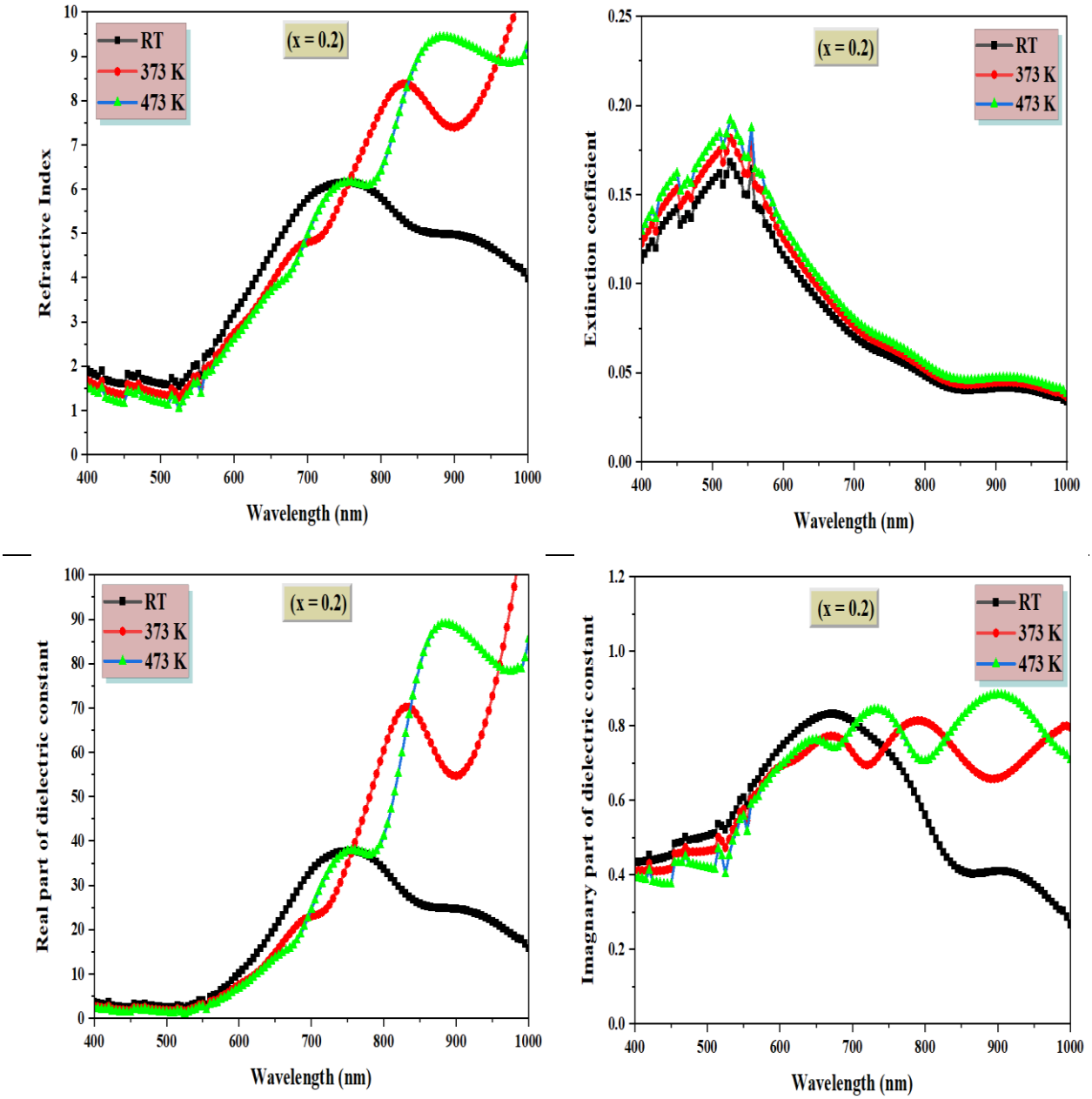


**Figure 4.** The fluctuation in The optical factors (refractive index, Extinction coefficient, real and imaginary components of dielectric constants) with wavelength for $ZnIn_2(Se_{0.8}Te_{0.2})_4$ with temperatures (R.T, 373 and 473) K.

Depending on the calculated absorption coefficients, the extinction coefficient was calculated using the relationship (7), It is the amount of attenuation in the intensity of the radiation electromagnetism, it represents the amount of energy absorbed into the thin films. We notice that the extinction coefficient exhibits a progressive increase as the energy of the photon increases, followed by a rapid increase in high photon energies, this indicates that there is an increase in absorption, in turn, led to an increase in the absorption coefficient, at annealing temperatures. We notice that the curves generally behave the same as above with the absorption edge towards

low photon energies, this confirms that the annealing temperatures have a clear effect to increase the extinction coefficient (35). **Figure 4** represents the change in refractive index as a function of wavelengths of $ZnIn_2(Se_{0.8}Te_{0.2})_4$ at (R.T, 373 and 473) K film; The refractive index curve closely resembles the nature of reflection. according to the link of reflexive index and reflection, and **Table 3** shows the refractive index value for all films with constant wavelength 500 nm (Within the visible range) The drop in the values of n during annealing can be attributed to the reduction in corresponding reflection resulting from structural and compositional changes that occur throughout the annealing process. This finding is consistent with previous studies (5,17). The relationship between the real ($\varepsilon_r$) & imaginary ($\varepsilon_i$) components of the dielectric constants is influenced by the values of n and k. At a wavelength of 500 nm, the values of $\varepsilon_r$ and $\varepsilon_i$ decrease due to the similarity in behavior between $\varepsilon_r$ and n; the behavior of $\varepsilon_i$ closely resembles that of k, primarily dependent on the k value. It is worth noting that the value of $\varepsilon_i$ is smaller than that of the thin film at room temperature, indicating a small dielectric loss. The optimal optical temperatures were observed at an annealing temperature of 473 K.

## 4. Conclusion

In this research many conclusions were reached: Possibility of $ZnIn_2(Se_{0.8}Te_{0.2})_4$ films using the thermal evaporation method, the film of the polycrystalline type, and when increasing annealing temperatures resulted in low displacement in the spectrum curve towards high values of angle diffraction. The nature of electronic transitions for all films was (allowed) direct transition electronic, the energy gap decreases with increasing annealing temperatures, the evaluation of all films showed an energy range of 1.7-1.6 eV, indicating their suitability for creating a junction in a solar cell., increasing annealing temperatures led to a change in the position of the peak of the curve transmittance and absorption towards photon energies are low, which indicates increased absorbency. The extinction coefficient increases due to an increased absorption coefficient.

## Acknowledgment

We thank the Thin Film Lab., Department of Physics, College of Education for Pure Science /Ibn Al-Haitham, University of Baghdad.

## Conflict of Interest

Conflict of Interest. The authors declare that they have no conflicts of interest.

## Funding

We hereby confirm that all the Figures and Tables in the manuscript are ours.

## Ethical Clearance

The project was approved by the local ethical committee at the University of Baghdad.

## References


1. Mohanty A, Priyambada A, Parida P, Ganguli B. Structural and electronic properties of Mn substituted ZnIn2Se4 chalcopyrite type semiconductor. Mater Today Proc. 2022;62 Part 2:1122–5. https://doi.org/10.1016/j.matpr.2022.04.323
2. Lopez-Rivera SA, Martinez L, Briceno-Valero JM, Echeverria R, De Armengol GG. Growth and photoconductivity properties of CdIn2Te4 and Cd0.83In0.34Te1.34. Prog Cryst Growth Charact. 1984;10:297–305. https://doi.org/10.1016/0146-3535(84)90048-0
3. Ouahrani T, Reshak AH, Khenata R, Baltache H, Amrani B, Bouhemadou A. Structural, electronic, linear, and nonlinear optical properties of ZnCdTe2 chalcopyrite. Phys Status Solidi Basic Res. 2011;248(3):712–8. http://dx.doi.org/10.1016/j. comm atsci. 2010. 09.030
4. Dhruv DK, Patel BH., Agrawal N, Banerjee R, Dhruv SD, Patel PB. Synthesis, electrical transport mechanisms and photovoltaic characteristics of p-ZnIn2Se4/n-CdTe thin film heterojunction. J Mater Sci Mater Electron. 2022;33(31):24003–15. https://doi.com/ article/10 .1007 /s10854-022-08755-z
5. Cai Y, Luo F, Guo Y, Guo F, Shi W, Yang S. Near-Infrared Light Driven ZnIn2S4-Based Photocatalysts for Environmental and Energy Applications: Progress and Perspectives. Molecules. 2023;28(5):2-15. https://doi.org/10.3390%2Fmolecules28052142
6. Dhruv DK, Patel BH. Fabrication and electrical characterization of Al/p-ZnIn2Se4 thin film Schottky diode structure. Mater Sci Semicond Process. 2016;54:29–35. http://dx. doi.org/10.1016/j. mssp. 2016.06.012
7. Lu Y, Jia X, Ma Z, Li Y, Yue S, Liu X. W5+–W5+ Pair Induced LSPR of W18O49 to Sensitize ZnIn2S4 for Full-Spectrum Solar-Light-Driven Photocatalytic Hydrogen Evolution. Adv Funct Mater. 2022;32(35):2203638. https://doi.org/10.1002/adfm. 202203 638
8. El-Nahass MM, Attia AA, Salem GF, Ali HAM., Ismail MI. Effect of vacuum annealing and substrate temperature on structural and optical properties of ZnIn2Se4 thin films. Phys B Condens Matter. 2013;425:23–30. http://dx.doi.org/10.1016/j.physb.2013.05.012
9. Yadav SP, Shinde PS, Rajpure KY, Bhosale CH. Preparation and properties of spray-deposited ZnIn2Se4 nanocrystalline thin films. J Phys Chem Solids. 2008;69(7):1747–52. https://doi .org/10. 1016/j.jpcs.2007.12.012
10. Choe SH. Optical energy gaps of undoped and Co-doped ZnIn2Se4 single crystals. Curr Appl Phys. 2009;9(1):1–3. https://doi.org/10.1016/j.cap.2007.10.083
11. Babu P, Ramakrishna Reddy KT, Miles RW. Precursor concentration effect on the properties of ZnIn2Se4 layers grown by chemical bath deposition. Energy Procedia. 2011;10:177–81. https://doi. org /10. 1016/j. egypro.2011.10.173
12. Bhalerao AB, Wagh BG, Shinde NM, Jambure SB, Lokhande CD. Crystalline zinc indium selenide thin film electrosynthesis and its photoelectrochemical studies. Energy Procedia. 2014;54:549–56. https://doi.org/10.1016/j.egypro.2014.07.296
13. Trah HP, Krämer V. Crystal structure of zinc indium selenide, ZnIn2Se4. Zeitschrift für Krist. 1985;173(3–4):199–203. https://doi/10.1524/ zkri. 1985.173. 14.199/pdf
14. Mamedova IA. Photoluminescence properties of ZnIn2Se4. Azerb J Phys. 2021;27(2):8–11.
15. El-Nahass MM, Attia AA, Ali HAM, Salem GF, Ismail MI. Nature of electrical transport properties of nanocrystalline ZnIn2Se4 thin films. Chaos, Solitons & Fractals. 2017;95:52–6. https://doi.org/10.1016/j.chaos.2016.12.005
16. Bozhko VV, Novosad OV, Parasyuk OV, Vainorius N, Sakaviciues A, Janonis V. Specific features of the low-temperature conductivity and photoconductivity of CuInSe2-ZnIn2Se4 alloys. Semiconductors. 2014;48(6):727–732. https://doi .org/10.1134/S10637826 14060086

17. Bozhko VV, Novosad AV, Parasyuk OV, Khyzhun OY, Vainorius N, Nekro A. Electrical properties and electronic structure of Cu1-xZnxInSe2 and Cu1-xZnxInS2 single crystals. J Phys Chem Solids. 2015;82:42–9. https: //doi.org/ 10.1016/ j.jpcs.2015.02.012
18. Yu F, Meng X, Cheng J, Liu J, Yao Y, Li J. Novel n-type thermoelectric material of ZnIn2Se4. J Alloys Compd. 2019;797:940–4. https://doi.org/10.1016/j.jallcom.2019.05.238
19. Sampath H, Jayaraj TI, Oommen R, Parthasarathy UR. Preparation and characterization of ZnIn2S4 thin film. Emerg Mater Res. 2015;4(2):286–9. https://doi.org /10.1680 /jemmr. 15.00023
20. Madelung O, Rössler U, Schulz M. Ternary Compounds, Organic Semiconductors. Landolt-börnstein-gr III Condens Matter; 2000. ISBN: 9783540667810
21. Khudayer IH, Hussien BH. Study of Some Structural and Optical Properties of AgAlSe2 Thin Films. I HJ PAS. 2016;29(2):41–51. https://www.iasj .net/iasj/ download/ d06fb 3c 7d8db8a28
22. Al-Maiyaly BKH. characterization of n-CdO: Mg/p-Si heterojunction dependence on annealing temperature. Ibn AL-Haitham J Pure Appl Sci. 2017;29(3):14–25. https://jih.uobaghdad. Edu .iq/ index.php/j/article/view/8
23. Hübschen G, Altpeter I, Tschuncky R, Herrmann HG. Materials characterization using nondestructive evaluation (NDE) methods. 2nd ed. Woodhead publishing; 2016. ISBN: 9780081000571
24. Athab RH, Hussein BH. Fabrication and investigation of zinc telluride thin films. Chalcogenide Lett. 2023;20(7):477–85. https://doi.org/10.15251/CL.2023.207.477
25. Hussein BH, Khudayer IH, Mustafa MH, Shaban AH. Effect of V, In and Cu doping on properties of p-type ZnSe/Si heterojunction solar cell. Prog Ind Ecol An Int J. 2019;13(2):173–86. https://doi.Org /10.1504/PIE.2019.099358
26. Hussein BH, Hassun HK. GROWTH AND OPTOELECTRONIC PROPERTIES OF p-CuO:Al/n-Si HETEROJUNCTION. J Ovonic Res. 2020;16(5):267–71. https://chalcogen.ro/ 267-Maiyaly BKH .pdf
27. Hussein BH, Hassun HK, Maiyaly BK, Aleabi SH. Effect of copper on physical properties of CdO thin films and n-CdO: Cu/p-Si heterojunction. J Ovonic Res. 2022;18:37–42. https://doi.org/10.15 251/JOR.2022.181.37
28. Sze SM, Li Y, Ng KK. Physics of semiconductor devices. 3rd ed. John Wiley & sons; 2021. ISBN: 9780470068328, https://doi.org/10.1002/0470068329.
29. Schroder DK. Semiconductor material and device characterization. 3rd ed. John Wiley & Sons; 2005. ISBN:9780471749097, https://doi.org/10.1002/0471749095.
30. Hussein WS, Fadhil AA, Aadim KA. Influence of laser energy and annealing on structural and optical properties of CdS films prepared by laser-induced plasma. Iraqi J Sci. 2020;61(6):1307–12. https://doi.org/10.24996/ijs.2020.61.6.8
31. Kim K, Ahn SK, Choi JH, Yoo J, Eo YJ, Cho JS. Highly efficient Ag-alloyed Cu (In, Ga) Se2 solar cells with wide bandgaps and their application to chalcopyrite-based tandem solar cells. Nano Energy. 2018;48:345–52. https://doi.org/10.1016/j.nanoen.2018.03.052
32. Ahmed GS, Hussein BH, Hassun HK, Salman EMT, Athab RH. Fabrication and Improvement of Optoelectronic Properties of Copper Chalcogenide Thin Films. Iraqi J Appl Phys. 2023;19(4):223–8. https://doi.www.iasj.net/iasj/article/284872
33. Tigau N, Ciupina V, Prodan G, Rusu GI, Gheorghies C, Vasile E. The influence of heat treatment on the electrical conductivity of antimony trioxide thin films. J Optoelectron Adv Mater. 2003;5(4):907–12. https://doi.old.joam.inoe.ro/arhiva/pdf5_4/Tigau.pdf
34. Sobhi SN, Hussein BH. Study the Influence of Antimony Dopant and Annealing on Structural, Optical and Hall Parameters of AgInSe2 Thin Film. Ibn AL-Haitham J Pure Appl Sci. 2022;35(3):16–24. https://doi.org/10.30526/35.3.2824

35. Athab RH, Hussein BH. Growth and Characterization of Vacuum Annealing AgCuInSe2 Thin Film. Ibn AL-Haitham J Pure Appl Sci. 2022;35(4):45–54. https://doi.org /10 .30526/ 35.4.2868